

# Higher-order contributions to the Rashba-Bychkov effect with application to Bi/Ag(111) surface alloy

Sz. Vajna<sup>1</sup>, E. Simon<sup>1,2</sup>, A. Szilva<sup>1</sup>, K. Palotas<sup>1</sup>, B. Ujfalussy<sup>3</sup>, and L. Szunyogh<sup>1\*</sup>

<sup>1</sup>*Department of Theoretical Physics, Budapest University of Technology and Economics, Budafoki út 8., H-1111 Budapest, Hungary*

<sup>2</sup>*Lóránd Eötvös University, Department of Physics, H-1518 Budapest POB 32, Hungary*

<sup>3</sup>*Hungarian Academy of Sciences, Institute for Solid State Physics and Optics, H-1525 Budapest, PO Box 49 H-1525 Hungary*

(Dated: September 26, 2021)

In order to explain the anisotropic Rashba-Bychkov effect observed in several metallic surface-state systems, we use  $k \cdot p$  perturbation theory with a simple group-theoretical analysis and construct effective Rashba Hamiltonians for different point groups up to third order in the wavenumber. We perform relativistic *ab initio* calculations for the  $(\sqrt{3} \times \sqrt{3})R30^\circ$  Bi/Ag(111) surface alloy and from the calculated splitting of the band dispersion we find evidence of the predicted third-order terms. Furthermore, we derive expressions for the corresponding third-order Rashba parameters to provide a simple explanation to the qualitative difference concerning the Rashba-Bychkov splitting of the surface states at Au(111) and Bi/Ag(111).

PACS numbers: 71.15.Rf 73.20.At 75.70.Tj

## I. INTRODUCTION

Since the first experimental verification by LaShell *et al.*<sup>1</sup> the spin-orbit induced splitting of Shockley states on metallic surfaces called the Rashba-Bychkov (RB) effect<sup>2</sup> became into the focus of experimental and theoretical research. These investigations range from the prototypical  $L$ -gap surface states at Au(111) and Ag(111)<sup>3-7</sup> and also at Au(110),<sup>8-10</sup> through Li/W(110) and Li/Mo(110) overlayers,<sup>11</sup> and the Gd(0001) surface,<sup>12</sup> to a large number of metallic surfaces and surface alloys related to Bi, Pb or Sb where the  $5p$  and  $6p$  orbitals show a pronounced spin-orbit splitting.<sup>13-28</sup> This huge interest is mainly triggered by potential spintronics applications in relation to the Datta-Das transistor,<sup>29</sup> the spin Hall effect<sup>30</sup> and the anomalous Hall effect.<sup>31</sup>

While accurate *ab initio* calculations satisfactorily account for most features of the measured dispersion relations of metallic surface states, there is an obvious need to explain the RB effect in terms of simple models containing a few, easily identifiable parameters. The simplest effective Hamiltonian of a two-dimensional electron gas, subject to spin-orbit interaction (SOI), includes in addition to the kinetic energy,  $\varepsilon_0 + \frac{\hbar^2 \mathbf{k}^2}{2m^*}$  ( $\mathbf{k}$  and  $m^*$  being the wavevector and the effective mass of the electrons, respectively), a Rashba term,<sup>2,32</sup>

$$H_R(\mathbf{k}) = \alpha_R (k_x \sigma_y - k_y \sigma_x), \quad (1)$$

where  $\alpha_R$  is the so-called Rashba parameter and  $\sigma_i$  ( $i = x, y, z$ ) denote the Pauli matrices. The corresponding eigenvalues,  $\varepsilon_{\pm}(\mathbf{k}) = \varepsilon_0 + \frac{\hbar^2 \mathbf{k}^2}{2m^*} \pm \alpha_R k$  ( $k = |\mathbf{k}|$ ) show an isotropic splitting for  $\mathbf{k} \neq 0$ , and, at least for moderate values of  $k$ , they readily can be fit to most experimental and *ab initio* dispersion relations.

Although not yet detected experimentally,<sup>8</sup> a RB splitting that is anisotropic in  $k$ -space is obvious for the surface states at Au(110). The  $C_{2v}$  point-group symmetry<sup>33</sup>

of the system not only implies an anisotropy of the effective mass,  $m_x^* \neq m_y^*$ , but, as discussed in terms of  $k \cdot p$  perturbation theory,<sup>10,35</sup> it leads to a Rashba Hamiltonian containing two independent Rashba parameters,  $\alpha_R^1$  and  $\alpha_R^2$ ,

$$H_R(\mathbf{k}) = \alpha_R^1 k_x \sigma_y + \alpha_R^2 k_y \sigma_x. \quad (2)$$

Fully relativistic *ab initio* calculations confirmed the existence of the anisotropic RB splitting at Au(110),<sup>9</sup> matching with a high accuracy to the eigenvalues of the effective Hamiltonian in Eq. (2).<sup>10</sup>

Even in case of high symmetry surfaces, i.e., having a point-group of  $C_{3v}$  or  $C_{4v}$ , several studies<sup>13,15,18,24,26,27</sup> called the attention to an anisotropic RB splitting. In Ref. 34 the anisotropic RB effect at Bi/Ag(111) and Pb/Ag(111) surfaces was reproduced by using a nearly-free electron model and explained due to in-plane structural inversion asymmetry. From the group-theoretical analysis in Ref. 35 it is, however, clear that under  $C_{3v}$  and  $C_{4v}$  point-group symmetry an effective  $2 \times 2$  Hamiltonian that is linear in the components of  $\mathbf{k}$  must be of the form of Eq. (1), hence, it can not explain the observed anisotropy of the RB splitting. Thus, we conclude that in these systems the anisotropic RB effect can be described by a Hamiltonian containing at least third-order polynomials of  $k_x$  and  $k_y$ . It should be noted that the second-order terms are related to the kinetic energy (effective mass terms) that are irrelevant to the RB splitting.

To construct Rashba Hamiltonians up to third order in  $k$ , in the present work we use  $k \cdot p$  perturbation theory and group-theoretical methods different from Ref. 35. Our analysis of the effective Hamiltonian is closely related to that of Ref. 36, where, for the case of  $C_{3v}$  symmetry, the correct form of  $H(\mathbf{k})$  is derived up to third order in  $k$  and the corresponding band dispersion was used to explain the hexagonal warping of the surface states' Fermi

contour observed experimentally in the topological insulator  $\text{Bi}_2\text{Te}_3$ .<sup>37</sup>

We also perform relativistic ab initio calculation for the  $\text{Bi}/\text{Ag}(111)$  ordered alloy in  $(\sqrt{3} \times \sqrt{3})R30^\circ$  superstructure and confirm that for higher values of  $k$ , but still in the measured range, third-order terms of the Rashba Hamiltonian are needed to reproduce the RB splitting and that these terms are of the predicted form. Moreover, using explicit expressions of the third-order Rashba parameters within  $k \cdot p$  perturbation theory and calculated spectral densities at the Brillouin zone center we are able to give a simple explanation why the  $\text{Au}(111)$  and the  $\text{Bi}/\text{Ag}(111)$  surface states exhibit isotropic and anisotropic RB splitting, respectively.

## II. PERTURBATION THEORY AND SYMMETRY ANALYSIS

Let  $\mathbf{Q}$  be a high symmetry point of the surface Brillouin zone (SBZ), for which a pair of spin-degenerate eigenstates exists on a nonmagnetic surface. Due to time reversal symmetry, this is always the case if  $\mathbf{Q} = -\mathbf{Q} + \mathbf{K}$  is satisfied where  $\mathbf{K}$  is a two-dimensional (2D) reciprocal-lattice vector. Such points are the center of the SBZ ( $\bar{\Gamma}$ ) and some special points at the boundary of SBZ such as the  $\bar{X}$ ,  $\bar{Y}$  and  $\bar{S}$  points for a primitive rectangular lattice, the  $\bar{M}$  and  $\bar{X}$  points for a square lattice and the  $\bar{M}$  point for a hexagonal lattice. As what follows, our investigations will concern solely this case termed as the proper Rashba effect.<sup>9</sup> As pointed out in Ref. 9, due to double-group symmetry there can happen degeneracy at points of the SBZ that doesn't meet the above condition, like the  $\bar{K}$  point for a hexagonal lattice (improper Rashba effect).

To describe the surface band around  $\mathbf{Q}$  it is worth to label the corresponding Bloch states by the wavenumber with respect to  $\mathbf{Q}$ ,  $\psi_{\mathbf{Q}+\mathbf{k}}$ , and introduce a new wavefunction,  $\phi_{\mathbf{k}}$  as

$$\psi_{\mathbf{Q}+\mathbf{k}}(\mathbf{r}) = e^{i\mathbf{k}\mathbf{r}} \phi_{\mathbf{k}}(\mathbf{r}), \quad (3)$$

with the boundary condition,  $\phi_{\mathbf{k}}(\mathbf{r} + \mathbf{T}) = e^{i\mathbf{Q}\mathbf{T}} \phi_{\mathbf{k}}(\mathbf{r})$ , where  $\mathbf{T}$  is a 2D real-lattice vector. Considering the Hamilton operator,  $\mathcal{H} = \frac{\mathbf{p}^2}{2m} + V + \mathcal{H}_{SO}$ , with the crystal potential,  $V$ , and  $\mathcal{H}_{SO}$  denoting the spin-orbit interaction,

$$\mathcal{H}_{SO} = \frac{\hbar}{4m^2c^2} (\nabla V \times \mathbf{p}) \cdot \boldsymbol{\sigma}, \quad (4)$$

the wavefunctions  $\phi_{\mathbf{k}}$  satisfy the eigenvalue equation,

$$(\mathcal{H}_0(\mathbf{k}) + \mathcal{H}_{SO}(\mathbf{k})) \phi_{\mathbf{k}} = \varepsilon(\mathbf{k}) \phi_{\mathbf{k}}, \quad (5)$$

with

$$\mathcal{H}_0(\mathbf{k}) = \frac{(\hbar\mathbf{k} + \mathbf{p})^2}{2m} + V, \quad (6)$$

and

$$\mathcal{H}_{SO}(\mathbf{k}) = \frac{\hbar}{4m^2c^2} (\nabla V \times (\hbar\mathbf{k} + \mathbf{p})) \cdot \boldsymbol{\sigma}. \quad (7)$$

Following the recipe used in Ref. 10, in the first step we look for the solution of the Schrödinger equation,

$$\mathcal{H}_0(\mathbf{k})\phi_{\mathbf{k}}^0 = \varepsilon_0(\mathbf{k})\phi_{\mathbf{k}}^0, \quad (8)$$

which can be elucidated, e.g. in terms of  $k \cdot p$  perturbation theory. Although such a calculation provides with a deeper insight into the problem,<sup>10</sup> in this section we just make use of the symmetry properties of the solutions,  $\varepsilon_0(\mathbf{k})$  and  $\phi_{\mathbf{k}}^0$ . First we note that since  $\mathcal{H}_0(\mathbf{k})$  is independent of the spin, the solutions of Eq. (8) remain degenerate in spin-space. Time reversal symmetry,  $T\mathcal{H}_0(\mathbf{k})T^{-1} = \mathcal{H}_0(-\mathbf{k})$  with  $T\psi = \psi^*$ , then immediately implies

$$\varepsilon_0(-\mathbf{k}) = \varepsilon_0(\mathbf{k}), \quad (9)$$

$$\phi_{-\mathbf{k}}^0 = (\phi_{\mathbf{k}}^0)^*, \quad (10)$$

where the phase of  $\phi_{\mathbf{k}}^0$  has been fixed without loss of generality. Clearly from Eq. (9), a polynomial form of  $\varepsilon_0(\mathbf{k})$  contains just even powers: the first non-trivial (second-order) terms are obviously related to the effective masses.

We can draw further relations from point-group symmetry. Let  $G_{\mathbf{Q}}$  be the small group of  $\mathbf{Q}$ , i.e.  $g\mathbf{Q} = \mathbf{Q} + \mathbf{K}$  for any  $g \in G_{\mathbf{Q}}$  and  $\mathbf{K}$  denoting an appropriate reciprocal-lattice vector. Using the standard definition for the action of a symmetry operation,  $(g \circ f)(\mathbf{r}) = f(g^{-1}\mathbf{r})$ , from the symmetry of the Hamilton operator,  $g \circ \mathcal{H}_0(\mathbf{k}) = \mathcal{H}_0(g\mathbf{k})$ , one easily can derive

$$\varepsilon_0(g\mathbf{k}) = \varepsilon_0(\mathbf{k}), \quad (11)$$

$$g \circ \phi_{\mathbf{k}}^0 = \phi_{g\mathbf{k}}^0. \quad (12)$$

In the second step, using  $\mathcal{H}_{SO}(\mathbf{k})$  as perturbation and  $\phi_{\mathbf{k}}^0 \chi_s$  with  $\chi_s$  being spinor eigenfunctions ( $s = \pm \frac{1}{2}$ ) as unperturbed wavefunctions, first-order degenerate perturbation theory is applied. The Rashba Hamiltonian,  $H_R(\mathbf{k})$ , is defined as the corresponding  $2 \times 2$  matrix,

$$H_R(\mathbf{k}) = \boldsymbol{\alpha}(\mathbf{k}) \cdot \boldsymbol{\sigma}, \quad (13)$$

where

$$\boldsymbol{\alpha}(\mathbf{k}) = \langle \phi_{\mathbf{k}}^0 | \frac{\hbar}{4m^2c^2} (\nabla V \times (\hbar\mathbf{k} + \mathbf{p})) | \phi_{\mathbf{k}}^0 \rangle. \quad (14)$$

Our present goal is to derive the polynomial form of  $\boldsymbol{\alpha}(\mathbf{k})$ . To this end we note two symmetry properties that can be obtained from Eqs. (10) and (12):

$$\boldsymbol{\alpha}(-\mathbf{k}) = -\boldsymbol{\alpha}(\mathbf{k}), \quad (15)$$

stating that  $\alpha_i(k_x, k_y)$  can be expanded in terms of polynomials of odd power and

$$\boldsymbol{\alpha}(g\mathbf{k}) = \det(g) g\boldsymbol{\alpha}(\mathbf{k}), \quad (16)$$

where  $\det(g) = 1$  for proper rotations and  $\det(g) = -1$  for improper rotations. Eq. (16) is then used to set up linear equations for the coefficients,  $c_i^l$ , of the  $n^{\text{th}}$ -order polynomials of  $\alpha_i(k_x, k_y) = \sum_{l=1, \dots, n} c_i^l k_x^l k_y^{n-l}$  ( $i = x, y, z$ ). Solving this set of linear equations serves to search for the vanishing coefficients, in principle, for any power  $n$ , hence, to determine the form of  $H_R(\mathbf{k})$ .

Another systematic way to obtain  $H_R(\mathbf{k})$  relies on the observation that Eq. (16) can be used to formulate the invariance of the Rashba Hamiltonian as

$$H_R(\mathbf{k}) = \boldsymbol{\alpha}(g\mathbf{k}) \cdot (\det(g)g\boldsymbol{\sigma}), \quad (17)$$

also implying that  $\boldsymbol{\sigma}$  transforms as an axial vector. Sort-

ing out the components of  $\mathbf{k}$  and  $\boldsymbol{\sigma}$  according to irreducible representations of  $G_{\mathbf{Q}}$ , their direct products can again be decomposed into irreducible representations. Eq. (17) states that only the total symmetric irreducible representations from this decomposition can contribute to  $H_R(\mathbf{k})$ . From the corresponding tables of the point groups<sup>33</sup> one can easily construct the possible terms entering  $H_R(\mathbf{k})$  according to increasing powers of  $k_x$  and  $k_y$ . In the Appendix this procedure is illustrated for the simple case of point group  $C_{2v}$ . As one of the main result of this work, in Table I we list the possible terms up to third order in  $k$  that can enter  $H_R(\mathbf{k})$  for different point groups relevant to surfaces of crystals.

$C_{hx}$	$C_2$	$C_3$	$C_4$	$C_{2v}$	$C_{3v}$	$C_{4v}$
$k_x\sigma_y,$ $k_y\sigma_x,$ $k_y\sigma_z$	$k_x\sigma_x,$ $k_x\sigma_y,$ $k_y\sigma_x,$ $k_y\sigma_y$	$k_x\sigma_x + k_y\sigma_y,$ $k_x\sigma_y - k_y\sigma_x$	$k_x\sigma_x + k_y\sigma_y,$ $k_x\sigma_y - k_y\sigma_x$	$k_x\sigma_y,$ $k_y\sigma_x$	$k_x\sigma_y - k_y\sigma_x$	$k_x\sigma_y - k_y\sigma_x$
$k_x^3\sigma_y,$ $k_x^2k_y\sigma_x,$ $k_x^2k_y\sigma_z,$ $k_xk_y^2\sigma_y,$ $k_y^3\sigma_x,$ $k_y^3\sigma_z$	$k_x^3\sigma_x,$ $k_x^3\sigma_y,$ $k_x^2k_y\sigma_x,$ $k_x^2k_y\sigma_y,$ $k_xk_y^2\sigma_x,$ $k_xk_y^2\sigma_y,$ $k_y^3\sigma_x,$ $k_y^3\sigma_y$	$(k_x^3 + k_xk_y^2)\sigma_x +$ $(k_x^2k_y + k_y^3)\sigma_y,$ $(k_x^3 + k_xk_y^2)\sigma_y -$ $(k_x^2k_y + k_y^3)\sigma_x,$ $(k_x^3 - 3k_xk_y^2)\sigma_z,$ $(k_y^3 - 3k_y^2k_x)\sigma_z$	$k_x^3\sigma_x + k_y^3\sigma_y,$ $k_x^3\sigma_y - k_y^3\sigma_x,$ $k_x^2k_y\sigma_x - k_xk_y^2\sigma_y,$ $k_xk_y^2\sigma_x + k_x^2k_y\sigma_y$	$k_x^3\sigma_y,$ $k_x^2k_y\sigma_x,$ $k_xk_y^2\sigma_y,$ $k_y^3\sigma_x$	$(k_x^3 + k_xk_y^2)\sigma_y -$ $(k_x^2k_y + k_y^3)\sigma_x,$ $(k_x^3 - 3k_xk_y^2)\sigma_z$	$k_x^3\sigma_y - k_y^3\sigma_x,$ $k_x^2k_y\sigma_x - k_xk_y^2\sigma_y$

TABLE I. Possible terms of the Rashba Hamiltonian for different point groups (first row) containing first-order (second row) and third-order (third row) polynomials of  $k_x$  and  $k_y$ .

Finally in this section, we comment on the method used in Ref. 35. In this work a Hamiltonian including SOI but excluding all  $k$ -dependent terms was considered as the unperturbed system and the twofold degenerate solutions,  $\phi_1$  and  $\phi_2$ , corresponding to the wavenumber  $\mathbf{Q}$  as the unperturbed solutions. The perturbation was therefore taken as  $\mathcal{H}'(\mathbf{k}) = \frac{\hbar}{m}\mathbf{k}\mathbf{p} + \frac{\hbar^2}{4m^2c^2}(\nabla V \times \mathbf{k}) \cdot \boldsymbol{\sigma}$  and, similar to our strategy, first-order degenerate perturbation theory was applied. The form of the effective Rashba Hamiltonian,  $H'_{ij}(\mathbf{k}) = \langle \phi_i | \mathcal{H}'(\mathbf{k}) | \phi_j \rangle$  ( $i, j = 1, 2$ ), is then determined via the invariance conditions,

$$H'(g\mathbf{k}) = D(g) H'(\mathbf{k}) D(g)^{-1}, \quad (18)$$

where  $D(g)$  is a  $2 \times 2$  unitary double-point group representation of  $g$ . In case of Abelian point groups ( $C_{hx}$ ,  $C_2$ ,  $C_3$  and  $C_4$ ), the degenerate states form time-reversed pairs and  $D(g)$  can simply be set up from the characters of the corresponding one-dimensional irreducible representations. Following from the definition of  $H'(\mathbf{k})$ , in Ref. 35 the first-order Rashba Hamiltonians were obtained for the groups  $C_{hx}$ ,  $C_{2v}$ ,  $C_{3v}$  and  $C_{4v}$ . It is, how-

ever, straightforward to show that, when applied to the Hamiltonian (13), Eq. (18) is equivalent with condition (17),<sup>38</sup> hence, using double-group representations leads to the same results as listed in Table I.

### III. THIRD-ORDER RASHBA SPLITTING AT BI/AG(111)

By using the relativistic Screened Korrington-Kohn-Rostoker (KKR) method<sup>39</sup> we performed calculations for the  $(\sqrt{3} \times \sqrt{3})R30^\circ$  ordered surface alloy Bi/Ag(111) to obtain a quantitative verification of our prediction of a third-order Rashba Hamiltonian. A 2D lattice constant of 2.892 Å related to fcc Ag bulk and, according to geometry optimization we performed in terms of the VASP method<sup>40</sup> and also in agreement to previous LAPW calculations,<sup>19</sup> an outward buckling of 36 % (0.85 Å) for the Bi atoms were considered. The local spin-density approximation as parametrized by Vosko *et al.*<sup>41</sup> was applied, the effective potentials and fields were

treated within the atomic sphere approximation with an angular momentum cut-off of  $\ell_{max} = 2$ . The energy integrations were performed by sampling 12 points on a semi-circular path in the upper complex semi-plane and for the necessary  $k$ -integrations we selected 36  $k$ -points in the irreducible segment of the surface Brillouin zone.

The calculated dispersion relation of the Bi surface states below the Fermi level is shown in Fig. 1 along the  $\bar{\Gamma} - \bar{M}$  direction of the SBZ. The maxima of the Rashba-split Bi  $sp_z$  band are shifted from the  $\bar{\Gamma}$  point by  $k_0 = 0.1 \text{ \AA}^{-1}$  and, using a parabolic fit around the maxima, we obtained an effective mass of  $m^* = -0.36 m_e$ . These values are in good agreement with experimental data,  $k_0 = 0.13 \text{ \AA}^{-1}$  and  $m^* = -0.35 m_e$ .<sup>18</sup> It should, however, be mentioned that the calculated surface bands are shifted downwards by about 0.5 eV as compared to experiment, most probably, due to the angular momentum cutoff and to the atomic sphere approximation used in the calculations. The Bi  $p_x p_y$  surface bands, shifted upwards due to crystal field splitting and to spin-orbit coupling, can also be clearly seen in Fig. 1.

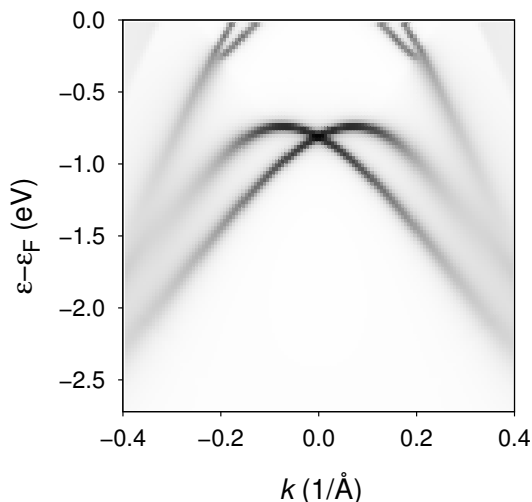


FIG. 1. Calculated dispersion relations of the occupied surface states of Bi/Ag(111) along the  $\bar{\Gamma} - \bar{M}$  direction of the SBZ.

In case of  $C_{3v}$  symmetry the effective Rashba Hamiltonian can be written up to third order in  $k$  as (see Table I),

$$H_R(\underline{k}) = (\alpha_1 + \alpha_3^1 k^2) (k_x \sigma_y - k_y \sigma_x) + a_3^2 k^3 \cos 3\varphi \sigma_z, \quad (19)$$

with the polar coordinate  $\varphi = \arccos(k_x/k)$ . Note that the  $x$  axis was chosen along the  $\bar{\Gamma} - \bar{K}$  direction of the SBZ. Obviously, there are two kinds of third-order contributions to the Hamiltonian (19): an isotropic one with coefficient  $\alpha_3^1$  and an anisotropic one with the coefficient  $\alpha_3^2$ . The square of the splitting of the eigenvalues,  $\Delta\varepsilon(\mathbf{k}) = (\varepsilon_+(\mathbf{k}) - \varepsilon_-(\mathbf{k}))/2$ , can then be expressed as

$$\Delta\varepsilon(\mathbf{k})^2 = (\alpha_1 k + \alpha_3^1 k^3)^2 + (\alpha_3^2)^2 k^6 \cos^2 3\varphi. \quad (20)$$

In Fig. 2 we plotted  $\Delta\varepsilon(\mathbf{k})^2$  along the  $\bar{\Gamma} - \bar{K}$  and the  $\bar{\Gamma} - \bar{M}$  directions, together with different fitting functions related to Eq. (20). It can be seen that a parabolic fit (dots),  $\alpha_1 k^2$  with  $\alpha_1 = 1.74 \text{ eV \AA}$ , applies well to the two curves only for about  $k < 0.07 \text{ \AA}^{-1}$ . Up to  $k \sim 0.13 \text{ \AA}^{-1}$  the two curves still coincide, however, the isotropic third-order contribution is needed for a good fit: here we used a fitting function  $(\alpha_1 k + \alpha_3^1 k^3)^2$  with the same value for  $\alpha_1$  as before and  $\alpha_3^1 = -14.2 \text{ eV \AA}^3$ . For wavenumbers  $k > 0.13 \text{ \AA}^{-1}$ , the anisotropy of the RB splitting becomes apparent: along  $\bar{\Gamma} - \bar{M}$  ( $\varphi = \pi/2$ ) the previous fit applies, while along  $\bar{\Gamma} - \bar{K}$  ( $\varphi = 0$ ) the fitting function had to be extended by the anisotropic term,  $(\alpha_3^2)^2 k^6$  with  $\alpha_3^2 = 9.4 \text{ eV \AA}^3$ . Our numerical results thus clearly support the appearance of third-order terms for the surface states of Bi/Ag(111) consistent with the functional form as derived from group-theoretical methods.

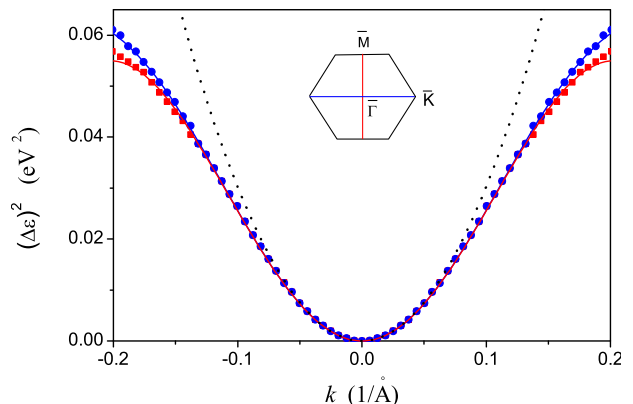


FIG. 2. Square of the calculated splitting,  $\Delta\varepsilon(\mathbf{k}) = (\varepsilon_+(\mathbf{k}) - \varepsilon_-(\mathbf{k}))/2$ , of the occupied surface states of Bi/Ag(111). Squares:  $\bar{\Gamma} - \bar{K}$  direction, circles:  $\bar{\Gamma} - \bar{M}$  direction, see the sketch of the SBZ in the inset. Dotted and solid lines display first-order and third-order fits as described in the text.

#### IV. COMPARISON OF THE RASHBA EFFECT AT AU(111) AND BI/AG(111)

It is well-known from experiments and ab initio calculations,<sup>1,3-6</sup> that the Au(111)  $L$ -gap surface states show a highly isotropic (first-order) Rashba splitting. Since both systems, Au(111) and Bi/Ag(111), exhibit  $C_{3v}$  symmetry, the question naturally arises why there is a remarkable difference concerning third-order RB splitting. In order to find, at least, a qualitative understanding of the problem we extended the  $k \cdot p$  perturbation calculations presented in Ref. 10 for the case of  $C_{2v}$  symmetry to  $C_{3v}$  symmetry and found the following expres-

sions for the third-order coefficients in Eq. (19),

$$\alpha_3^1 = \frac{\hbar^4}{4m^4c^2} \sum_{n,m} \frac{\langle \phi_0 | p_x | \phi_n^+ \rangle \langle \phi_n^+ | \partial_z V | \phi_m^+ \rangle \langle \phi_m^+ | p_x | \phi_0 \rangle}{(\varepsilon_0 - \varepsilon_n^E)(\varepsilon_0 - \varepsilon_m^E)}, \quad (21)$$

and

$$\alpha_3^2 = \frac{\hbar^4}{4m^4c^2} \sum_{n,m} \frac{\langle \phi_0 | p_x | \phi_n^+ \rangle \langle \phi_n^+ | \partial_x V | \phi_m^- \rangle \langle \phi_m^- | p_x | \phi_0 \rangle}{(\varepsilon_0 - \varepsilon_n^E)(\varepsilon_0 - \varepsilon_m^E)}. \quad (22)$$

From the above formulas it turns out that third-order corrections to the effective Hamiltonian arise from an admixture between the surface state,  $\phi_0$  of  $sp_z$  orbital character at energy  $\varepsilon_0$ , and those corresponding to the two-dimensional irreducible representation,  $E$ ,  $\phi_n^\pm$  with  $p_x \pm ip_y$  character, at energy  $\varepsilon_n^E$ . Note that all these states are eigenstates of the Hamiltonian,  $\mathcal{H} = \frac{p^2}{2m} + V$ , at the center of the surface band  $\mathbf{Q}$ . It is remarkable that, similar to the isotropic first-order Rashba parameter, the strength of the isotropic contribution,  $\alpha_3^1$ , depends on the partial derivative of the crystal potential normal to the surface,  $\partial_z V$ , while the coefficient for the anisotropic term,  $\alpha_3^2$ , is related to the in-plane gradient of the potential,  $\partial_x V$ .

In Fig. 3 we plotted the scalar-relativistic, orbital projected partial densities of states (Bloch spectral functions) at the  $\bar{\Gamma}$  point in an appropriate energy window around the surface states of Au(111) and Bi/Ag(111). From the upper panel it can be seen that in case of Au(111) the edge of the bulk subband of  $E$  symmetry closest to the surface state is by  $\Delta\varepsilon = 1.77$  eV below  $\varepsilon_0$ . The situation is entirely different for Bi/Ag(111), since the Bi  $p_x p_y$  states of  $E$  symmetry are separated from the  $sp_z$  state by only  $\Delta\varepsilon = 0.27$  eV. Since these are the characteristic energy differences that enter the denominators in Eqs. (21) and (22), a difference of at least two orders in magnitude can indeed be estimated concerning the third-order RB effect. Most probably, the actual values of the matrixelements of  $p_x$  and  $\partial_{x,z} V$  even further strengthen this difference.

## V. CONCLUSIONS

Based on  $k \cdot p$  perturbation theory including spin-orbit interaction we gave a suitable definition to an effective Hamiltonian, Eqs. (13) and (14), describing the Rashba-Bychkov splitting on metallic surfaces. Due to time reversal and point-group symmetry we showed how to obtain the most general forms for the effective Hamiltonian, and derived them up to third order in  $k$  for point groups compatible with surfaces of real crystals. Since the effective Hamiltonian (13) applies to a couple of non-interacting two-band models, the expressions listed in Table I can be used in quite a general sense.

Using the relativistic Screened Korringa-Kohn-Rostoker method, we demonstrated that the Rashba splitting of the Bi  $sp_z$  surface band of the ordered surface

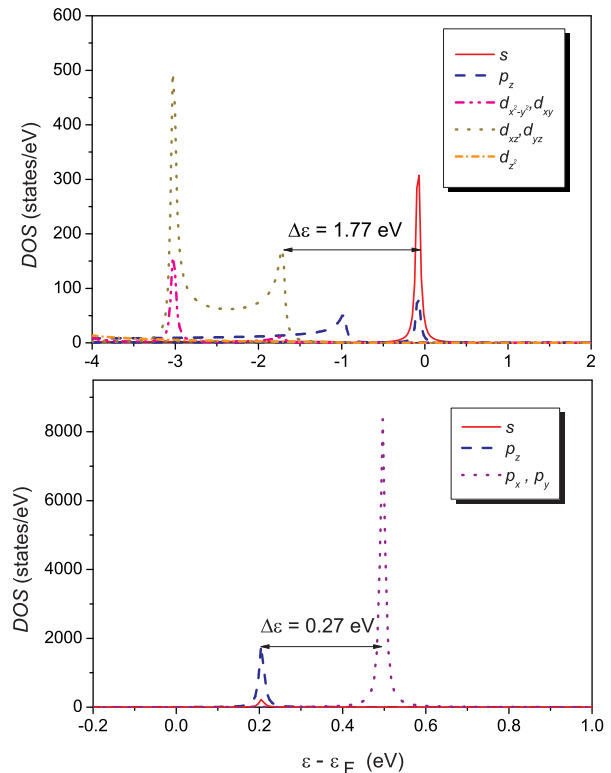


FIG. 3. Calculated orbital projected partial densities of states at the  $\bar{\Gamma}$  point around the surface states of Au(111) (upper panel) and Bi/Ag(111) (lower panel).

alloy Bi/Ag(111) can not be satisfactorily described in terms of a first-order isotropic Rashba Hamiltonian. Moreover, we showed that the strong third-order contribution is subject to an anisotropy consistent with the dispersion relation deduced from our symmetry analysis.

We also derived explicit formulas for the third-order anisotropy parameters and established that the isotropic and anisotropic contributions are related to the normal-to-plane and the in-plane gradients of the crystal potential, respectively. Comparing the energy separation of relevant orbital projected bands for Au(111) and Bi/Ag(111), the derived expressions were useful to give a qualitative understanding of the different nature of Rashba-Bychkov splitting in these two systems.

## ACKNOWLEDGMENTS

The authors appreciate stimulating discussions with Gergely Zarand. Financial support was provided by the Hungarian Research Foundation (contract no. OTKA K77771, K84078 and PD83353) and by the New Széchenyi Plan of Hungary (Project ID: TÁMOP-4.2.1/B-09/1/KMR-2010-0002). K.P. kindly acknowledges support of the Bolyai Grant.

## Appendix: Rashba Hamiltonians for point group $C_{2v}$

By using the direct products of irreducible representations, in this Appendix we give an example for the polynomial forms of a  $2 \times 2$  effective Hamiltonian for the point-group  $C_{2v}$ . Let us denote the elements of the group by  $E : \{x, y, z\}$ ,  $C_2 : \{-x, -y, -z\}$ ,  $S_x : \{-x, y, z\}$  and  $S_y : \{x, -y, z\}$ . The group has four one-dimensional irreducible representations:  $A_1$ ,  $A_2$ ,  $B_1$ ,  $B_2$  with the character table,<sup>33</sup>

	$E$	$C_2$	$S_x$	$S_y$
$A_1$	1	1	1	1
$A_2$	1	1	-1	-1
$B_1$	1	-1	-1	1
$B_2$	1	-1	1	-1

Making use that the  $\mathbf{k}$  and  $\boldsymbol{\sigma}$  transform as polar and axial vectors, respectively, a comparison with the character table lets us to sort out the components of this vectors according to irreducible representations:  $B_1 : k_x, \sigma_y$ ,  $B_2 : k_y, \sigma_x$  and  $A_2 : \sigma_z$ .

From the table of direct products,

	$A_1$	$A_2$	$B_1$	$B_2$
$A_1$	$A_1$	$A_2$	$B_1$	$B_2$
$A_2$		$A_1$	$B_2$	$B_1$
$B_1$			$A_1$	$A_2$
$B_2$				$A_1$

it is easy to find that the only combinations that are first order in  $k_x$  and  $k_y$  and correspond to the  $A_1$  irreducible representations are  $k_x \sigma_y$  and  $k_y \sigma_x$ , therefore, the first-order Rashba Hamiltonian can be written in the form of Eq. (2).

The second-order polynomials of  $k_x$  and  $k_y$  can be sorted according to irreducible representations as follows:  $A_1 : k_x^2, k_y^2$  and  $A_2 : k_x k_y$ . It should be noted that this implies the form of  $\frac{\hbar^2}{2m_x^*} k_x^2 + \frac{\hbar^2}{2m_y^*} k_y^2$  for the effective mass term. The third-order polynomials of  $k_x$  and  $k_y$  can then be classified as  $B_1 : k_x^3, k_x k_y^2$  and  $B_2 : k_y^3, k_y k_x^2$ . Taking direct products with  $\sigma_i$  of  $A_1$  symmetry leads to the possible third-order contributions to the Rashba Hamiltonian:  $k_x^3 \sigma_y$ ,  $k_x^2 k_y \sigma_x$ ,  $k_x k_y^2 \sigma_y$  and  $k_y^3 \sigma_x$ , i.e.

$$H_R^3(\mathbf{k}) = \alpha_3^1 k_x^3 \sigma_y + \alpha_3^2 k_x^2 k_y \sigma_x + \alpha_3^3 k_x k_y^2 \sigma_y + \alpha_3^4 k_y^3 \sigma_x. \quad (\text{A.1})$$

\* szunyogh@phy.bme.hu

- <sup>1</sup> S. LaShell, B.A. McDougall, and E. Jensen, Phys. Rev. Lett. **77**, 3419 (1996).
- <sup>2</sup> Y.A. Bychkov and E.I. Rashba, J. Phys. C **17**, 6039 (1984).
- <sup>3</sup> G. Nicolay, F. Reinert, S. Hüfner, and P. Blaha, Phys. Rev. B **65**, 033407 (2001).
- <sup>4</sup> J. Henk, A. Ernst, and P. Bruno, Phys. Rev. B **68**, 165416 (2003).
- <sup>5</sup> J. Henk, M. Hoesch, J. Osterwalder, A. Ernst, and P. Bruno, J. Phys.: Condens. Matter, **16**, 7581 (2004).
- <sup>6</sup> R. Mazzarello, A. Dal Corso, and E. Tosatti, Surface Science **602**, 803 (2008).
- <sup>7</sup> A. Nuber, J. Braun, F. Forster, J. Minár, F. Reinert, and H. Ebert, Phys. Rev. B **83**, 165401 (2011).
- <sup>8</sup> A. Nuber, M. Higashiguchi, F. Forster, P. Blaha, K. Shimada, and F. Reinert, Phys. Rev. B **78**, 195412 (2008).
- <sup>9</sup> M. Nagano, A. Kodama, T. Shishidou, and T. Oguchi, J. Phys.: Condens. Matter **21**, 064239 (2009).
- <sup>10</sup> E. Simon, A. Szilva, B. Ujjfalussy, B. Lazarovits, G. Zarand, and L. Szunyogh, Phys. Rev. B **81** 235438 (2010).
- <sup>11</sup> E. Rotenberg, J. W. Chung, and S. D. Kevan, Phys. Rev. Lett. **82**, 4066 (1999).
- <sup>12</sup> O. Krupin, G. Bihlmayer, K. Starke, S. Gorovikov, J.E. Prieto, K. Döbrich, S. Blügel, and G. Kaindl, Phys. Rev. B **71**, 201403 (2005).
- <sup>13</sup> Yu.M. Koroteev, G. Bihlmayer, J.E. Gayone, E.V. Chulkov, S. Blügel, P.M. Echenique, and Ph. Hofmann, Phys. Rev. Lett. **93**, 046403 (2004).
- <sup>14</sup> Ph. Hofmann, J. E. Gayone, G. Bihlmayer, Yu. M. Koroteev, and E. V. Chulkov, Phys. Rev. B **71**, 195413 (2005).
- <sup>15</sup> K. Sugawara, T. Sato, S. Souma, T. Takahashi, M. Arai, and T. Sasaki, Phys. Rev. Lett. **96**, 046411 (2006).

- <sup>16</sup> T. Hirahara, T. Nagao, I. Matsuda, G. Bihlmayer, E.V. Chulkov, Yu.M. Koroteev, P. M. Echenique, M. Saito, and S. Hasegawa, Phys. Rev. Lett. **97**, 146803 (2006).
- <sup>17</sup> D. Pacilé, C. R. Ast, M. Papagno, C. Da Silva, L. Moreschini, M. Falub, Ari P. Seitsonen, and M. Grioni, Phys. Rev. B **73**, 245429 (2006).
- <sup>18</sup> C.R. Ast, J. Henk, A. Ernst, L. Moreschini, M.C. Falub, D. Pacilé, P. Bruno, Kl. Kern, and M. Grioni, Phys. Rev. Lett. **98**, 186807 (2007).
- <sup>19</sup> G. Bihlmayer, S. Blügel, and E.V. Chulkov, Phys. Rev. B **75**, 195414 (2007).
- <sup>20</sup> C.R. Ast, G. Wittich, P. Wahl, R. Vogelgesang, D. Pacilé, M.C. Falub, L. Moreschini, M. Papagno, M. Grioni, and K. Kern, Phys. Rev. B **75**, 201401(R) (2007).
- <sup>21</sup> J.H. Dil, F. Meier, J. Lobo-Checa, L. Patthey, G. Bihlmayer, and J. Osterwalder, Phys. Rev. Lett. **101**, 266802 (2008).
- <sup>22</sup> C.R. Ast, D. Pacilé, L. Moreschini, M.C. Falub, M. Papagno, K. Kern, M. Grioni, J. Henk, A. Ernst, S. Ostanin, and P. Bruno, Phys. Rev. B **77**, 081407(R) (2008).
- <sup>23</sup> T. Hirahara, T. Komorida, A. Sato, G. Bihlmayer, E. V. Chulkov, K. He, I. Matsuda, and S. Hasegawa, Phys. Rev. B **78**, 035408 (2008).
- <sup>24</sup> L. Moreschini, A. Bendouan, I. Gierz, C. R. Ast, H. Mirhosseini, H. Höchst, K. Kern, J. Henk, A. Ernst, S. Ostanin, F. Reinert, and M. Grioni, Phys. Rev. B **79**, 075424 (2009).
- <sup>25</sup> L. Moreschini, A. Bendouan, H. Bentmann, M. Assig, K. Kern, F. Reinert, J. Henk, C. R. Ast, and M. Grioni, Phys. Rev. B **80**, 035438 (2009).
- <sup>26</sup> I. Gierz, B. Stadtmüller, J. Vuorinen, M. Lindroos, F. Meier, J. Hugo Dil, K. Kern, and C. R. Ast, Phys. Rev. B

- 81**, 245430 (2010).
- <sup>27</sup> H. Mirhosseini, I. V. Maznichenko, Samir Abdelouahed, S. Ostanin, A. Ernst, I. Mertig, and J. Henk, Phys. Rev. B **81**, 073406 (2010).
- <sup>28</sup> S. Abdelouahed and J. Henk, Phys. Rev. B **82**, 193411 (2010).
- <sup>29</sup> For a review, see I. Zutic, J. Fabian, and S. Das Sarma, Rev. Mod. Phys. **76**, 323-410 (2004).
- <sup>30</sup> J. Sinova, D. Culcer, Q. Niu, N. A. Sinitsyn, T. Jungwirth and A. H. MacDonald, Phys. Rev. Lett. **92**, 126603 (2004); J. Wunderlich, B. Kaestner, J. Sinova, and T. Jungwirth, Phys. Rev. Lett. **94**, 047204 (2005).
- <sup>31</sup> D. Culcer, A. MacDonald, Q. Niu, Phys. Rev. B **68**, 045327 (2003); V. K. Dugaev, P. Bruno, M. Taillefumier, B. Canals, and C. Lacroix, Phys. Rev. B **71**, 224423 (2005); T. S. Nunner, G. Zarand, and F. von Oppen, Phys. Rev. Lett. **100**, 236602 (2008).
- <sup>32</sup> L. Petersen and P. Hedegård, Surf. Sci. **459**, 49 (2000).
- <sup>33</sup> In this work we use the standard Schönflies notations for point-groups, see S. L. Altmann and P. Herzig, *Point-Group Theory Tables* (Clarendon Press, Oxford, 1984).
- <sup>34</sup> J. Prempfer, M. Trautmann, J. Henk, and P. Bruno, Phys. Rev. B **76**, 073310 (2007).
- <sup>35</sup> T. Oguchi and T. Shishidou, J. Phys.: Condens. Matter **21**, 092001 (2009).
- <sup>36</sup> Liang Fu, Phys. Rev. Lett. **103**, 266801 (2009).
- <sup>37</sup> Y. L. Chen, J. G. Analytis, J.-H. Chu, Z. K. Liu, S.-K. Mo, X. L. Qi, H. J. Zhang, D. H. Lu, X. Dai, Z. Fang, S. C. Zhang, I. R. Fisher, Z. Hussain, and Z.-X. Shen, Science **325**, 178 (2009).
- <sup>38</sup> Sz. Vajna, *Anisotropic Bychkov-Rashba effect on metallic surfaces* (in Hungarian), BSc Theses, Budapest University of Technology and Economics (2010).
- <sup>39</sup> J. Zabloudil, R. Hammerling, L. Szunyogh and P. Weinberger, *Electron Scattering in Solid Matter: a theoretical and computational treatise*, Springer Berlin Heidelberg New York, 2005.
- <sup>40</sup> G. Kresse and J. Hafner, Phys. Rev. B **47**, 558 (1993); *ibid.* **49**, 14 251 (1994); G. Kresse and J. Furthmüller, Comput. Mat. Sci. **6**, 15 (1996); G. Kresse and J. Furthmüller, Phys. Rev. B **54**, 11 169 (1996).
- <sup>41</sup> S. H. Vosko, L. Wilk, and M. Nusair, Can. J. Phys. **58**, 1200 (1980).